Long non-coding RNA BLACAT2/miR-378a-3p/YY1 feedback loop promotes the proliferation, migration and invasion of uterine corpus endometrial carcinoma

CHEN ZHANG[1], RUICONG WANG[2], MENGYUAN LI[1] and QING YANG[1]

[1]Department of Obstetrics and Gynecology, Shengjing Hospital of China Medical University, Shenyang, Liaoning 110004; [2]Department of Obstetrics and Gynecology, The First Affiliated Hospital of Dalian Medical University, Dalian, Liaoning 116011, P.R. China

Received August 16, 2022; Accepted March 24, 2023

DOI: 10.3892/or.2023.8544

Abstract. Uterine corpus endometrial carcinoma (UCEC) is a common gynecological malignancy with high rates of mortality and morbidity. The expression of long non-coding RNA bladder cancer-associated transcript 2 (BLACAT2) has been previously found to be aberrantly upregulated in UCEC. However, the regulatory consequences of this in UCEC progression remain poorly understood. In the present study, human UCEC cell lines AN3CA and HEC-1-A were infected with lentiviruses to overexpress BLACAT2 (Lv-BLACAT2) or knock down BLACAT2 using short hairpin RNA (Lv-shBLACAT2). BLACAT2 overexpression was found to promote the G_1/S transition of cell cycle progression and UCEC cell proliferation. In addition, BLACAT2 overexpression was observed to facilitate UCEC cell migration and invasion. By contrast, BLACAT2 knockdown resulted in inhibitory effects in UCEC cell physiology. BLACAT2 overexpression also contributed to the activation of the MEK/ERK pathway. Subsequently, BLACAT2 was demonstrated to bind to microRNA (miR)-378a-3p according to dual-luciferase assays, where it appeared to function as a sponge of miR-378a-3p in 293T cells. miR-378a-3p overexpression was found to suppress UCEC cell proliferation, invasion, and ERK activation. Lentivirus-mediated knockdown of its target, the transcription factor Yin Yang-1 (YY1), was observed to reverse the oncogenic effects of BLACAT2 overexpression. Furthermore, YY1 was found to bind to the promoter of BLACAT2, suggesting that YY1 can regulate BLACAT2 expression. To conclude, results from the present study suggest that BLACAT2, miR-378a-3p and YY1 can form a feedback loop instead of an unidirectional axis, which can in turn regulate UCEC tumorigenesis through the MEK/ERK pathway. The present study furthered the understanding of UCEC tumorigenesis and may provide novel therapeutic targets for UCEC treatment.

Correspondence to: Professor Qing Yang, Department of Obstetrics and Gynecology, Shengjing Hospital of China Medical University, 36 Sanhao Street, Shenyang, Liaoning 110004, P.R. China
E-mail: yangqing_sj@126.com

Abbreviations: lncRNAs, long non-coding RNAs; miRNAs, microRNAs; YY1, transcription factor Yin Yang-1; UCEC, uterine corpus endometrial carcinoma; RT-qPCR, reverse transcription-quantitative polymerase chain reaction; ChIP, chromatin immunoprecipitation; ERK, extracellular signal-regulated kinase

Key words: uterine corpus endometrial carcinoma, lncRNA-BLACAT2, miR-378a-3p, YY1, cell behavior

Introduction

Uterine corpus endometrial carcinoma (UCEC) is a malignancy that originates from the endometrium and is frequently symptomatic at advanced stage (1,2). It is one of the most common gynecological malignancies worldwide with increasing incidence (1,2). Patients with advanced disease present with abnormal bleeding in the vagina or pelvic organs (3). For women with localized disease on diagnosis, the 5-year survival rate is >90%, but the 5-year overall survival rate decreases to <20% in patients with distal metastases (4). Therefore, identifying novel therapeutic targets for UCEC is particularly important for treating patients with UCEC.

Long non-coding RNAs (lncRNAs) belong to a class of non-coding RNAs that are typically >200 nucleotides in length and have little or no protein-coding potential (5). LncRNAs reverse the inhibitory effects of microRNAs (miRNAs or miRs) on mRNAs by functioning as miRNA sponges (6). To date, numerous lncRNAs have been reported to be aberrantly expressed in various cancers, where lncRNAs serve pivotal regulatory roles in tumorigenesis and metastasis (7,8). Bladder cancer-associated transcript 2 (BLACAT2) was first identified to be an oncogene in bladder cancer, which increases tumor lymphangiogenesis and lymphatic metastasis (9,10). It has been previously reported that the expression of BLACAT2 is upregulated in several malignancies, including hepatocellular carcinoma, cervical cancer, and nasopharyngeal carcinoma (11-19), which suggests that BLACAT2 is closely associated with cancer progression. In fact, BLACAT2 has been demonstrated to aggravate hepatocellular carcinoma

via sponging miR-3619-5p, and plays a functional role in modulating radiotherapy resistance in cervical cancer (11,12). Previous RNA-sequencing analysis indicated that BLACAT2 expression is highly upregulated in the endometrium of patients with UCEC compared to adjacent normal controls (20). In addition, another previous study revealed that BLACAT2 is a possible oncogenic lncRNA in endometrial cancer (21). However, the regulatory mechanism underlying the role of BLACAT2 remains unclear.

Transcription factor Yin Yang-1 (YY1) is a zinc finger protein belonging to the GLI-Kruppel family (22). As a DNA-binding protein, it serves dual functions and has been documented to regulate cell differentiation, proliferation, apoptosis and cell division (23). YY1 can either function as an activator or repressor of gene transcription, depending on the context of YY1-binding proteins in proximity (24). Specifically, YY1 can bind to the promoter region of LINC00673, thereby increasing its transcription in *cis* (25). Numerous studies have demonstrated the upregulation of YY1 in ovarian, prostate, esophageal, and melanoma cancer (26-29). In addition, YY1 expression has also been demonstrated to be upregulated in human endometrioid endometrial adenocarcinoma cell lines and tumor tissues. YY1 knockdown can inhibit cell proliferation and migration in endometrioid endometrial carcinoma (EEC), whereas YY1 overexpression was found to promote EEC cell proliferation (30).

MicroRNAs (miRNAs or miRs) form another family of highly conserved non-coding RNAs, which are 20-25 nucleotides in length (31,32). They typically mediate translational repression or mRNA transcript degradation by targeting the 3'-untranslated region (UTR) of downstream mRNAs (31,32). An increasing number of miRNAs have been observed to regulate the progression of UCEC (33,34). In particular, miR-378a-3p has been recognized as a potential miRNA that can bind to BLACAT2 according to bioinformatic analysis. However, its function in UCEC remains unreported. Recently, BLACAT2 was revealed to bind to miR-378a-3p in bladder cancer cells, where it regulated cell viability, migration and invasion (35).

Based on previous studies and findings, it was hypothesized that BLACAT2 may serve an important biological function in UCEC by regulating miR-378a-3p and/or YY1. Therefore, the present study explored the possible functions of BLACAT2, YY1 and miR-378a-3p, in addition to their associations with UCEC progression.

Materials and methods

Clinical specimens. A total of 40 paired cancer-adjacent and UCEC tissue samples were obtained from January 2018 to December 2019 and frozen for further analysis. All volunteers (mean age, 57.78) provided written informed consent and the present study was approved (approval no. 2021PS723K) by the Ethics Committee of Shengjing Hospital of China Medical University (Shengjing, China) and in accordance with the Declaration of Helsinki. The inclusion and exclusion criteria were as follows: The patients with UCEC included in this study were diagnosed by histopathological detection. The tumor tissues and their adjacent normal tissues were collected by surgical resection. None of these patients received radiotherapy or chemotherapy before the surgery. The patients that had undergone non-curative resection, cancer recurrence, severe injury of vital organs or had a history of autoimmune diseases were excluded. The clinicopathological characterisitics of the patients with UCEC included in the present study are provided in Table I.

Cell lines and culture conditions. Human endometrial cancer cell lines Ishikawa (cat. no. iCell-h113), RL95-2 (cat. no. iCell-h182), HEC-1-B (cat. no. iCell-h084), AN3CA (cat. no. icell-h018), and HEC-1-A (cat. no. iCell-h083) were purchased from iCell Bioscience, Inc. Ishikawa, AN3CA, and HEC-1-B cells were grown in MEM medium (Beijing Solarbio Science & Technology Co., Ltd.). HEC-1-A cells were cultured in McCoy's 5A medium (Procell Life Science & Technology Co., Ltd.). RL95-2 cells were cultured in DMEM/F12 medium (Procell Life Science & Technology Co., Ltd.). All the culture media were supplemented with 10% FBS (Sangon Biotech Co., Ltd.) and cells were cultured in a CO_2 incubator at 37˚C.

Database analysis. Gene Expression Profiling Interactive Analysis (GEPIA; http://gepia.cancer-pku.cn/) was used to analyze the different expression of genes in various human cancers. There was a binding relationship between BLACAT2 and hsa-miR-378a-3p, as predicted by starBase (https://starbase.sysu.edu.cn/agoClipRNA.php?source=lncRNA). Furthermore, 49 target genes common to miRDB (http://www.mirdb.org/), TargetScan (https://www.targetscan.org/vert_72/) and starBase were identified. Jasper database (https://jaspar.genereg.net/) was utilized to show the association between YY1 and BLACAT2 promotor region.

Lentivirus packaging. The helper plasmids pSPAX2 and pMD2.G were obtained from Hunan Fenghui Biotechnology Co., Ltd. For lentivirus packaging, 293T cells (cat. no. ZQ0033; https://www.zqxzbio.com/Index/p_more/pid/486.html; Shanghai Zhong Qiao Xin Zhou Biotechnology Co., Ltd.) were cultured to a confluence of ~70% and then transfected with pSPAX2 (3 μg), pMD2.G (2.2 μg), and the plasmids with overexpressed BLACAT2/Negative control (5 μg) or shRNA against BLACAT2/YY1/Negative control (5 μg) using Lipofectamine® 3000 (Thermo Fisher Scientific, Inc.) at 37˚C according to the manufacturer's protocols. At 6 h post transfection, the culture medium of the cells was changed into fresh DMEM medium (Wuhan Servicebio Technology Co. Ltd.) with 10% FBS (37˚C and 5% CO_2). At 48 h post trasfection, the cell supernatant was harvested as packaged lentivirus and filtered through a 0.45-μm pore size filter.

Cell treatments. To establish the stable UCEC cell line with overexpressed BLACAT2 or knocked down BLACAT2, the AN3CA and HEC-1-A cells were selected and infected with the corresponsing lentiviruses at a multiplicity of infection (MOI) of 10. The puromycin (0.9 μg/ml) was used for stable cell line selection, while 0.3 μg/ml of puromycin was for maintenance.

To clarify the function of miR-378a-3p in UCEC, HEC-1-A cells were transfected with miR-378a-3p mimics (100 pmol) or negative control (NC; 100 pmol) mimics using Lipofectamine® 2000 (Invitrogen; Thermo Fisher Scientific, Inc.).

Table I. Clinicopathological characteristics of patients with uterine corpus endometrial carcinoma.

Patient No.	Age	Tumor stage (T)	Lymph node metastasis (N)	Distant metastasis (M)	TNM	Histo-pathological grade	Maximum tumor diameter (cm)	Tumor number
1	65	T1a	N1a	M0	IIIC1	G3	9	Multifocal
2	66	T1b	N0	M0	IB	G1	5.5	Unifocal
3	63	T1a	N0	M0	IA	G1-G2	3	Unifocal
4	60	T3b	N0	M0	IIIB	G3	4.5	Multifocal
5	45	T1a	N0	M0	IA	G1	1.1	Unifocal
6	77	T1a	N0	M0	IA	G1	6	Unifocal
7	53	T1a	N0	M0	IA	G1-G2	4.5	Unifocal
8	57	T1a	N0	M0	IA	G1	3.5	Unifocal
9	58	T1a	N0	M0	IA	G1-G2	3.1	Multifocal
10	48	T2	N0	M0	II	G1-G2	4	Multifocal
11	58	T1a	N0	M0	IA	G2	3.5	Unifocal
12	69	T1a	N0	M0	IA	G3	6	Unifocal
13	55	T1b	N0	M0	IB	G2-G3	2.0	Unifocal
14	68	T1b	N0	M0	IB	G1-G2	2.5	Unifocal
15	60	T1a	N0	M0	IA	G3	3.5	Unifocal
16	40	T1a	N0	M0	IA	G1	3.5	Unifocal
17	52	T2	N0	M0	II	G1	2.5	Unifocal
18	49	T1a	N0	M0	IA	G2	5.5	Unifocal
19	73	T1b	N0	M0	IB	G1-G2	3.5	Unifocal
20	46	T3b	N1a	M0	IIIC1	G1	7	Multifocal
21	67	T1a	N0	M0	IA	G2	6	Unifocal
22	65	T1a	N0	M0	IA	G1-G2	4	Unifocal
23	54	T1a	N0	M0	IA	G3	4.9	Multifocal
24	66	T1b	N0	M0	IB	G2-G3	4.5	Multifocal
25	54	T1a	N0	M0	IA	G2-G3	5	Unifocal
26	49	T2	N2a	M0	IIIC2	G1-G2	3.5	Multifocal
27	53	T1b	N0	M0	IB	G2-G3	4.7	Unifocal
28	54	T2	N0	M0	II	G1	5	Unifocal
29	70	T2	N0	M0	II	G2	7.5	Multifocal
30	65	T1a	N0	M0	IA	G2	4	Unifocal
31	54	T1a	N0	M0	IA	G2	1.6	Unifocal
32	67	T1b	N0	M0	IB	G1-G2	5.9	Unifocal
33	42	T1a	N0	M0	IA	G2	5.4	Unifocal
34	58	T2	N0	M0	II	G1-G2	9	Unifocal
35	60	T1a	N2a	M0	IIIC2	G2-G3	4.8	Multifocal
36	53	T1b	N0	M0	IB	G2	6.9	Unifocal
37	58	T1a	N0	M0	IA	G1	4.8	Unifocal
38	44	T1a	N0	M0	IA	G1	3.5	Unifocal
39	63	T1a	N0	M0	IA	G1	1.3	Multifocal
40	53	T1b	N0	M0	IB	G2	6	Unifocal

To investigate the role of YY1 in the regulation of BLACAT2 underlying UCEC development, AN3CA cells with stably overexpressed BLACAT2 were infected with lentivirus encoding shRNA against YY1 (Lv-shYY1) at a MOI of 10.

The shRNAs against BLACAT2, YY1 and NC were synthesized by General Biological System and inserted into the lentiviral vector. The sequence information used in the present study was as follows: shBLACAT2#1, 5'-GGTTAAGACATTTCTACAAAT-3'; shBLACAT2#2, 5'-GAGTGGAGAGACTCAGCTACC-3'; shYY1, 5'-CGACGACTACATTGAACAAAC-3'; shNC, 5'-TTCTCCGAACGTGTCACGT-3'; miR-378a-3p mimics sense, 5'-ACUGGACUUGGAGUCAGAAGGC-3'; NC mimics sense, 5'-UCACAACCUCCUAGAAAGAGUAGA-3'.

All cells after transfection were cultured at 37˚C and 5% CO_2. Overexpression/knockdown efficiency was assessed using reverse transcription-quantitative PCR (RT-qPCR).

RT-qPCR. UCEC cells (6x10^5/well; 6-well plate) or tumor tissues were lysed in TRIpure (BioTeke Corporation) to isolate the total RNAs. The miRNAs were reverse transcripted into cDNA using the miRNA First Strand cDNA Synthesis Kit according to the manufacturer's instructions (Sangon Biotech Co., Ltd.). LncRNA and mRNA were synthesized into cDNA via reverse transcription PCR. The thermocycling conditions for reverse transcription PCR were as follows: Step 1, a total of 12.5 μl reaction was prepared by adding 1 μg RNA, 1 μl oligo $(dT)_{15}$, 1 μl random primers, and ddH_2O. The reaction was incubated at 70˚C for 5 min and then placed on ice for 2 min; step 2, 2 μl dNTP, 4 μl 5X buffer, 0.5 μl Rnase inhibitor, and 1 μl Super M-MLV reverse transcriptase (BioTeke Corporation) were added into the reaction. The total reaction samples were then incubated at 25˚C for 10 min, 40˚C for 50 min, and 80˚C for 10 min.

The cDNAs were amplified and detected using 2X Power Taq PCR MasterMix (BioTeke Corporation) and SYBR Green fluorescence (SYBR Green qPCR kit; Sigma-Aldrich; Merck KGaA) on an Exicycler™ 96 Real-Time System (Bioneer Corporation). The thermocycling conditions for qPCR were as the following: Step 1, 94˚C for 5 min; step 2, 94˚C for 15 sec; step 3, 60˚C for 25 sec; step 4, 72˚C for 30 sec; scan and step 2, 40 cycles; step 5, 72˚C for 5 min 30 sec; step 6, 40˚C for 2 min 30 sec; step 7, melting 60-94˚C every 1.0˚C for 1 sec; and step 8, 25˚C for 1-2 min. The mRNA levels of the target genes were quantified using the $2^{-\Delta\Delta Cq}$ method (36). β-actin was the reference for the quantification of BLACAT2 and YY1. The reference gene U6 was used for miR-378a-3p quantification. Primers for the genes assessed were as follows: BLACAT2 forward, 5'-GAGGAGGAGAAGCAATCA-3' and reverse, 5'-GGAGCCCATCCATTAGAG-3'; YY1 forward, 5'-ACC CACGGTCCCAGAGT-3' and reverse, 5'-AAAGCGTTTCCC ACAGC-3'; miR-378a-3p forward, 5'-ACTGGACTTGGAGTC AGAAGGC-3'. All primers were synthesized by Genscript.

Western blot analysis. Proteins samples in cells or tumor tissues were extracted using cell lysis buffer (cat. no. P0013; Beyotime Institute of Biotechnology) supplemented with 1 mM phenylmethanesulfonyl fluoride (PMSF; Beyotime Institute of Biotechnology). Protein concentration was quantified using a BCA kit (Beyotime Institute of Biotechnology). Subsequently, 20-40 μg proteins in each lane were separated on the SDS-PAGE gel (11% or 8%). The 11 or 8% gel was respectively selected for protein separation according the molecular weight of the target proteins. The proteins were then transferred onto PVDF membranes and blocked with a 5% skimmed milk solution at room temperature for 1 h. The membranes were incubated with the primary antibodies against MMP2 (1:500; cat. no. 10373-2-AP; ProteinTech Group, Inc.), MMP9 (1:1,000; cat. no. 10375-2-AP; ProteinTech Group, Inc.), cyclin D1 (1:500; cat. no. A19038; ABclonal Biotech Co., Ltd.), cyclin E (1:1,000; cat. no. A14225; ABclonal Biotech Co., Ltd.), phosphorylated (p)-MEK1/2 (1:500; cat. no. AP0209; ABclonal Biotech Co., Ltd.), MEK1/2 (1:500; cat. no. AF6385; Affinity Biosciences, Ltd.), p-ERK1/2 (1:500; cat. no. AF1015; Affinity Biosciences, Ltd.) or ERK1/2 (1:500; cat. no. AF0155; Affinity Biosciences, Ltd.) overnight at 4˚C. This was followed by a 40-min incubation with the HRP-conjugated anti-rabbit and anti-mouse secondary antibodies (1:10,000; cat. no. A0208 and A0216, respectively; Beyotime Institute of Biotechnology) at 37˚C. Enhanced chemiluminescence (ECL)-detecting reagent (Beyotime Institute of Biotechnology) was then added onto the membrane, before the protein bands were visualized in WD-9413B gel-imaging system (Beijing LIUYI Biotechnology Co., Ltd.) and analyzed using Gel-Pro-Analyzer 4.0 software (Media Cybernetics, USA).

Dual-luciferase reporter assay. 293T cells (2x10^5/well; 12-well plate) were used for dual-luciferase reporter assay. To assess the potential association between miR-378a-3p and BLACAT2 or YY1, the wild-type BLACAT2 or 3'UTR of YY1 mRNA containing a putative binding site for miR-378a-3p and their corresponding mutant sequences were amplified and cloned into the pmirGLO plasmid (General Biological System). Vectors containing the wild-type or mutant sequence were co-transfected with miR-378a-3p mimics or NC mimics into 293T cells using Lipofectamine® 3000 at 37˚C using the established protocol. At 6 h post transfection, the culture medium was replaced by fresh DMEM (Wuhan Servicebio Technology Co., Ltd.) containing 10% FBS (Hangzhou Sijiqing Biological Engineering Materials Co., Ltd.). In total, 48 h after transfection, the activity of firefly luciferase in cells was detected using a Dual-Luciferase Reporter Gene Assay Kit (Nanjing KeyGen Biotech Co., Ltd.), which was normalized to that of *Renilla* luciferase.

Similarly, to assess the binding of YY1 to BLACAT2 promoter, three regions (-500+5, -1,000+5 and -1,500+5) in the BLACAT2 promoter or the YY1 coding sequence were inserted into the pmirGLO vector. Vectors encoding each of the BLACAT2 promoters were co-transfected with the vector encoding YY1 into 293T cells at 37˚C using the established protocol. The luciferase activity was detected at 48 h post transfection.

Cell counting kit-8 (CCK-8) assay. Cells (3x10^3/well)were seeded into a 96-well plate and cultured under standard conditions. Cell viability was measured at 0, 24, 48 and 72 h using the CCK-8 (Sigma-Aldrich; Merck KGaA) solution. In total, 800 μl CCK-8 was added into each well, before the cells were cultured for 1 h. The optical density of each well was then detected at 450 nm using a microplate reader (800Ts; BioTek Instruments, Inc.).

Flow cytometric analysis. Cell cycle distribution was revealed using a Cell Cycle and Apoptosis Detection kit (cat. no. C1052; Beyotime Institute of Biotechnology). After the fixing with cold 70% ethanol for 12 h at 4˚C, the cells were harvested by centrifugation at 4˚C for 3 min with a speed of 420 x g, and 500 μl dye buffer was added. Next, the cells were incubated with 25 μl of propidium iodide staining solution and 10 μl RNase A for 30 min at 37˚C. The percentage of the cells in G_1, S, and G2 phases were analyzed using a flow cytometer (NovoCyte; ACEA Bioscience, Inc.) and quantified using the software NovoExpress (version 1.5.0; Agilent Technologies, Inc.).

Wound healing assay. Cells were seeded into a six-well plate at a density of $5x10^5$/well and grown to a confluence of >95% at the start of the assay. The cells were then cultured in serum-free medium containing 1 μg/ml mitomycin C (Sigma-Aldrich; Merck KGaA) for 1 h. Subsequently, a 200-μl pipette tip was used to make a straight vertical scratch down through the cell monolayers. Cell debris were then removed and an image was recorded using an inverted phase-contrast microscope (IX53; Olympus Corporation). The cells were thereafter cultured in fresh serum-free medium at 37˚C and 5% CO_2 for 24 h. The images of wounds at 0 and 24 h were recorded, before the migration rate was calculated as: (Wound distance at 0 h-wound distance at 24 h)/wound distance at 0 h x100%.

Transwell assay. Cell invasion in AN3CA and HEC-1-A cells was assessed using Transwell assays with a 24-well Transwell chamber (Corning, Inc.). The chamber was pre-coated with Matrigel at 37˚C for 2 h (Corning, Inc.), which wasdiluted with serum-free mediumat a ratio of 1:3. The cells were then seeded into the pre-coated upper chamber in their serum-free culture medium at a density of $1.5x10^4$ cells/well. In total, 800 μl culture medium (MEM for AN3CA cells and McCoy's 5A for HEC-1-A) containing 10% FBS (Biological Iundustries) was added into the lower chamber. After 24 h of incubation at 37˚C, the cells were fixed with 4% paraformaldehyde for 20 min at room temperature and then stained with 0.1% crystal violet solution at room temperature for a further 5 min. A total of five fields of view were randomly selected for each chamber and the number of cells were counted under an inverted phase-contrast microscope (IX53; Olympus Corporation).

Gelatin zymography assay. MMP-2 and MMP-9 activity in AN3CA and HEC-1-A cells were determined using gelatin zymography as previously described (37). Total protein concentration in the culture supernatants was quantified with a BCA kit (Beyotime Insitute of Biotechnology). A total of 10 mg/ml gelatin (Sigma-Aldrich; Merck KGaA) was added to a 10% acrylamide separating gel. The proteins in the supernatants were separated using SDS-PAGE. The SDS-PAGE gel was washed twice for 40 min in an elution solution (2.5% Triton X-100, 50 mmol/l Tris-HCl, 5 mmol/l $CaCl_2$ and 1 μmol/l $ZnCl_2$; pH 7.6). The gel was then incubated in the developing buffer (50 mmol/l Tris-HCl, 5 mmol/l $CaCl_2$, 1 μmol/l $ZnCl_2$, 0.02% Brij and 0.2 mol/l NaCl) at 37˚C for 40 h. Following incubation, the gel was stained with a staining solution (0.5% Coomassie blue R250, 30% methanol and 10% glacial acetic acid; Beijing Solarbio Science & Technology Co., Ltd.) at room temperature for 3 h. Digestion bands were visualized using a Gel imaging system (WD-9413B; Beijing LIUYI Biotechnology Co., Ltd.) and analyzed with a microplate reader (ELX-800; BioTeke Corporation).

Chromatin immunoprecipitation (ChIP). The ChIP assay was conducted using a ChIP assay kit (cat. no. WLA106a; Wanleibio, Co., Ltd.) according to the manufacturer's protocol. Briefly, HEC-1-A cells were formaldehyde-crosslinked and then lysed using lysis buffer from Wanleibio, Co., Ltd. (cat. no. WLA106a). The chromatin of HEC-1-A cells was fragmented by sonication and collected, followed by the incubation with PBS-washed ProteinA+G beads (60 μl) on a rotator at 4˚C for 1-2 h. Following centrifugation with a speed of 625 x g at room temperature for 1 min, the cell supernatants were collected and 20 μl was used as the Input. The chromatin fragments (100 μl/group) were then incubated with the anti-YY1 antibody (2 μg, cat. no. 66281-1-Ig; ProteinTech Group, Inc.) on a rotator at 4˚C overnight. The PBS-washed ProteinA+G beads (60 μl) were next added and maintained on a rotator at 4˚C for 1-2 h. IgG (1 μg; ChIP assay kit; Wanleibio, Co., Ltd.) was used as a negative control antibody. The protein-DNA complexes were then washed using the wash buffer from Wanleibio, Co., Ltd. (cat. no. WLA106a) on a rotator at 4˚C for 10 min/time. The supernatant was removed using centrifugation at a speed of 625 x g at room temperature for 1 min. A total of 100 μl of elution buffer was added and incubated overnight at 65˚C to reverse cross-links. The DNA specimens released from the protein-DNA complexes were purified and analyzed using ChIP followed by PCR (ChIP-PCR; BioTeke Corporation) to amplify the promoter region of BLACAT2. The primer pair for the BLACAT2 promoter was as follows: Forward, 5'-AGTCTC ATTCTGTCGCCT-3' and reverse, 5'-TGTAATCCCAGCACT GTG-3'. PCR products were detected using electrophoresis on 2% agarose gel (Biowest).

In vivo tumorigenesis model. For the present study, 4-week-old female BALB/c nude mice weighing 16±1 g (n=6 per group, with a total of 24 mice) were purchased from Huafukang Biosciences and adaptively housed for a week under a controlled environment (humidity, 45-55%; temperature, 22±1˚C; and a 12-h day/night cycle), with free access to water and food. The mice were then randomly divided into four groups: Lv-NC (AN3CA), Lv-BLACAT2 (AN3CA), Lv-shNC (HEC-1-A), and Lv-shBLACAT2 (HEC-1-A) groups. AN3CA cells with stably overexpressed BLACAT2/NC and HEC-1-A cells with stably knocked down BLACAT2/NC ($1x10^7$ cells/100 μl) were subcutaneously injected into the right flank of the nude mice. The tumor size was measured every 4 days. A total of 4 weeks later, all mice were sacrificed by CO_2 asphyxiation. The flow displacement rate of CO_2 was 40% of the chamber volume per min. Death was confirmed by the cessation of movement, breathing and heartbeat. The tumor tissues were then separated and weighed, before they were fixed in 4% paraformaldehyde for further analysis. The tumor volumes were calculated according to the following formula: Volume=length x width^2 x0.5. The animal experiments were approved by the Ethics Committee of Shengjing Hospital of China Medical University (approval no. 2021PS741K). A tumor size of 20 mm at the largest diameter was permitted by the Ethics Committee. After 4 weeks, the maximum tumor diameter observed was not exceeded.

Immunohistochemistry. The tumor tissues fixed in 4% paraformaldehyde (at room temperature for 24 h) were embedded in paraffin and then sectioned into 5-μm slices. After dewaxing, rehydration, and antigen retrieval, the tumor slices were incubated with 3% H_2O_2 at room temperature for 15 min. Following 15 min of blocking with goat serum (Beijing Solarbio Science & Technology Co., Ltd.) at room temperature, tumor slices were incubated with a anti-Ki67 antibody (1:100 dilution; cat. no. A2094; ABclonal Biotech

Co., Ltd.) overnight at 4˚C. Subsequently, the sections were incubated with an HRP-conjugated secondary antibody (cat. no. 31460; Thermo Fisher Scientific, Inc.) at 37˚C for 1 h. The sections were then stained with diaminobenzidine (DAB; Beijing Solarbio Science & Technology Co., Ltd.) at room temperature for 5 min. Following DAB visualization, the sections were immersed into water and then re-stained using hematoxylin at room temperature for 3 min. The Ki67-positive cells were finally observed under a light microscope (BX53; Olympus Corporation).

Statistical analysis. Data were analyzed using the GraphPad Prism 8.0 software (GraphPad Software, Inc.) and the results are presented as the mean ± standard deviation. Statistical analyses were performed using one-way ANOVA followed by Tukey's multiple comparisons test, two-way ANOVA followed by Sidak's multiple comparisons test or unpaired Student's t-test. P<0.05 was considered to indicate a statistically significant difference.

Results

Expression of BLACAT2 in UCEC. BLACAT2 was found to be upregulated in cervical cancer, ovarian cancer and UCEC, whereas its expression was not found to be significantly different in breast cancer (Fig. 1A). Although carcinogenic functions have been previously identified in cervical cancer (38) and ovarian cancer (39), the role of BLACAT2 in UCEC remains unclear. BLACAT2 expression was therefore detected in clinical samples using RT-qPCR. BLACAT2 expression was found to be significantly increased in UCEC tumors compared with that in the adjacent normal tissues (P<0.01; Fig. 1B). Furthermore, RT-qPCR confirmed that BLACAT2 is expressed in human endometrial cancer cell lines Ishikawa, RL95-2, HEC-1-B, AN3CA and HEC-1-A (Fig. 1C).

BLACAT2 overexpression promotes the proliferation of UCEC cells. As revealed in Fig. 1C, AN3CA cells exhibited the lowest expression of BLACAT2 than that in the other UCEC cell lines, while HEC-1-A cells exhibited the highest expression of BLACAT2. Thus, AN3CA cells were selected for BLACAT2 overexpression, whereas HEC-1-A cells were selected for BLACAT2 knockdown. As the results of RT-qPCR revealed, the expression of BLACAT2 in AN3CA cells was higher when compared to the Lv-NC group, whereas that in HEC-1-A cells was significantly lower when compared to the Lv-shNC group (P<0.01; Fig. 2A). Cell viability was then detected using CCK-8 assay. Notably, BLACAT2 overexpression enhanced UCEC cell viability, whereas BLACAT2 knockdown reduced cell viability (P<0.01; Fig. 2B). Cell cycle progression was next investigated in these cells. BLACAT2 overexpression decreased cell accumulation in the G_1 phase and increased the number of cells in the S and G_2 phases. By contrast, there were more HEC-1-A cells in the G_1 phase and fewer cells in the S and G_2 phases following BLACAT2 knockdown (P<0.05; Fig. 2C). The expression of cyclin D1 and cyclin E, which are essential regulators of G_1/S transition during cell cycle progression (40), were found to be upregulated in UCEC cells following BLACAT2 overexpression. However, their protein expression levels were significantly reduced by BLACAT2 knockdown (P<0.01; Fig. 2D and E). Therefore, these data indicated that BLACAT2 overexpression promotes the proliferation of UCEC cells.

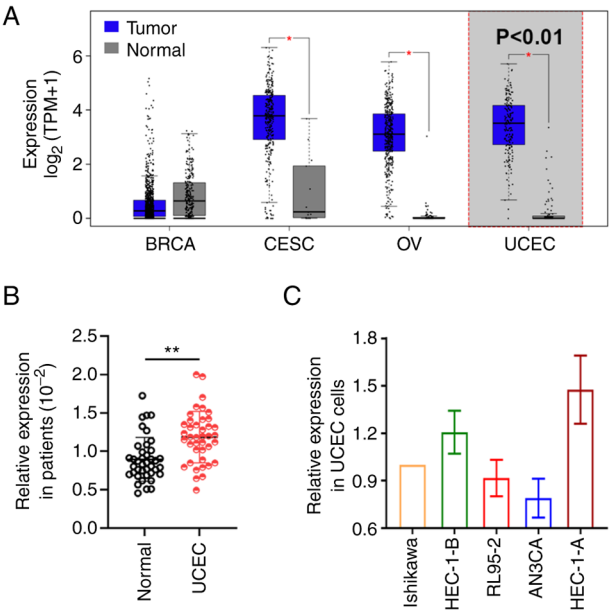

Figure 1. Expression of BLACAT2 in UCEC tumors and cell lines. (A) BLACAT2 expression level in BRCA, CESC, OV and UCEC using the GEPIA database. The expression of BLACAT2 in (B) 40 paired clinical specimens and in (C) the UCEC cell lines Ishikawa, HEC-1-B, RL95-2, AN3CA and HEC-1-A. *P<0.05 and **P<0.01 vs. normal. BLACAT2, bladder cancer-associated transcript 2; UCEC, uterine corpus endometrial carcinoma; BRCA, breast cancer; CESC, cervical cancer; OV, ovarian cancer.

BLACAT2 overexpression facilitates UCEC cell migration and invasion. The migration and invasion of AN3CA and HEC-1-A cells were subsequently assessed by wound healing and Transwell assays. BLACAT2 overexpression was observed to improve the migration rate of UCEC cells, whilst knockdown of BLACAT2 expression significantly inhibited the migration of these tumor cells (P<0.05; Fig. 3A). BLACAT2 appeared to mediate similar effects on UCEC cell invasion (P<0.01; Fig. 3B). MMP9 and MMP2 are proteins that can potentiate cancer cell invasion (41). Therefore, the present study next examined the protein expression levels of MMP9 and MMP2 in cells, and determined that BLACAT2 overexpression increased the expression of MMP9 and MMP2. By contrast, BLACAT2 knockdown inhibited their protein expression levels in UCEC cells (P<0.01; Fig. 3C). In addition, gelatin zymography assay revealed that BLACAT2 overexpression enhanced the activity of MMP9 and MMP2, whilst BLACAT2 knockdown weakened their activities (P<0.01; Fig. 3D). These findings indicated that BLACAT2 serves an important role in the migration and invasion of UCEC cells.

BLACAT2 overexpression enhances MER/ERK signaling in UCEC cells. The ERK signaling pathway has been reported to be aberrantly activated in cancer, which can promote cell proliferation and invasion (42). Therefore, the activation status of ERK and MEK in UCEC cells was assessed using western blotting (Fig. 4A and C). BLACAT2 overexpression was found to increase the phosphorylation of MEK1/2 and ERK1/2 without

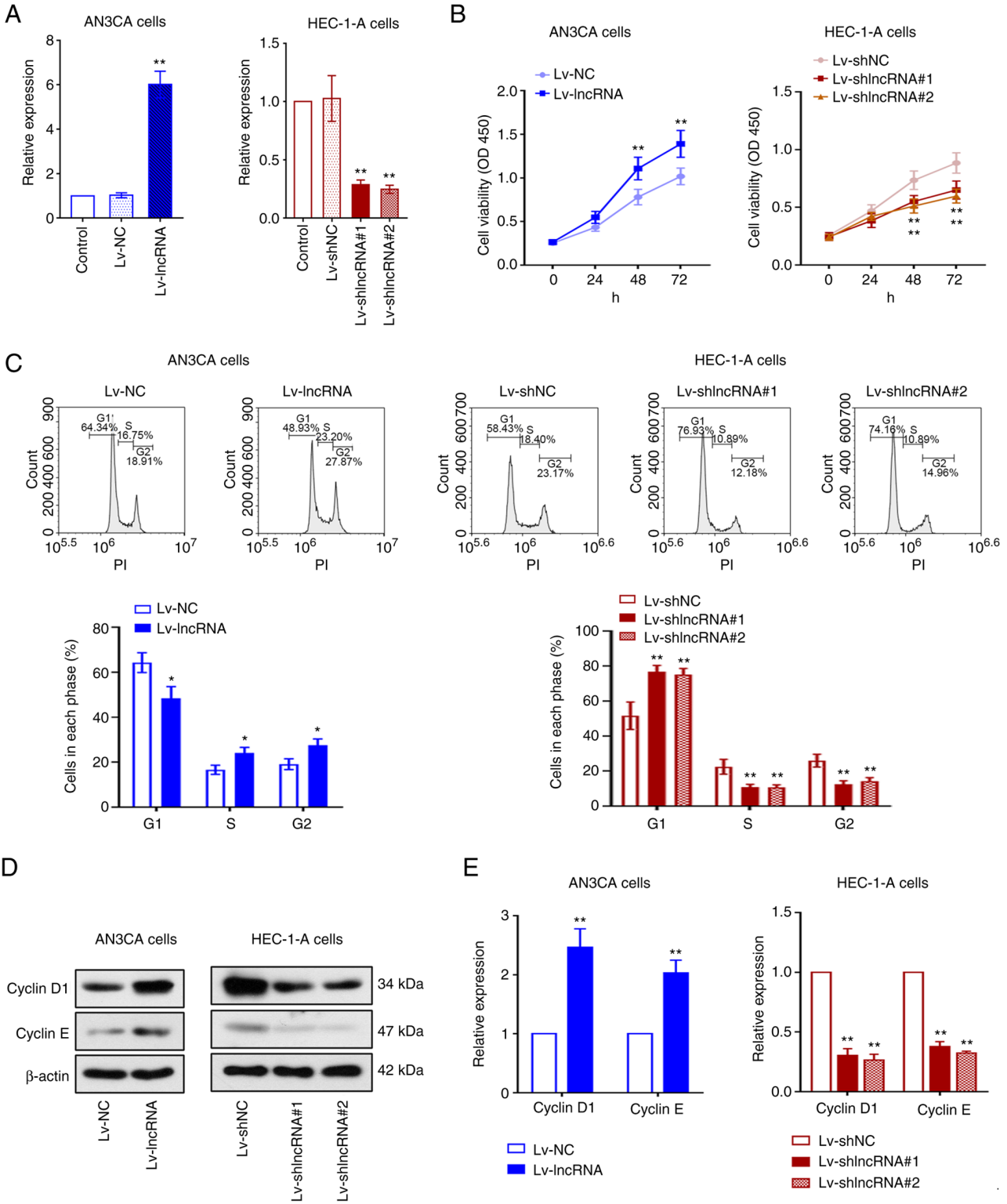

Figure 2. BLACAT2 promotes uterine corpus endometrial carcinoma cell proliferation by accelerating G1/S cell cycle progression. The AN3CA stable cell line with overexpressed BLACAT2 and the HEC-1-A cell stable cell line with knocked down BLACAT2 were established, respectively. (A) BLACAT2 expression in AN3CA and HEC-1-A cells was measured using reverse transcription-quantitative PCR. (B) Cell viability was determined using the Cell Counting Kit-8 assay. The vertical axis represented the value of optical density at 450 nm. (C) AN3CA and HEC-1-A cells at each phase (G1, S and G2) of the cell cycle were assessed using flow cytometry. (D) Representative images and (E) quantification of cyclin D1 and cyclin E expression in AN3CA and HEC-1-A cells. Values are presented as the means ± SD (n=3). *P<0.05 and **P<0.01 vs. Lv-NC or Lv-shNC. BLACAT2, bladder cancer-associated transcript 2; Lv, lentivirus; NC, negative control; sh, short-interfering.

altering the expression of their corresponding total protein in UCEC cells. The increased ratio of p-MEK1/2 or p-ERK1/2 to total MEK1/2 or total ERK1/2, respectively, suggested that the MEK/ERK pathway was activated by BLACAT2 overexpression (P<0.05; Fig. 4B). By contrast, BLACAT2 knockdown significantly suppressed the activation of this pathway in UCEC

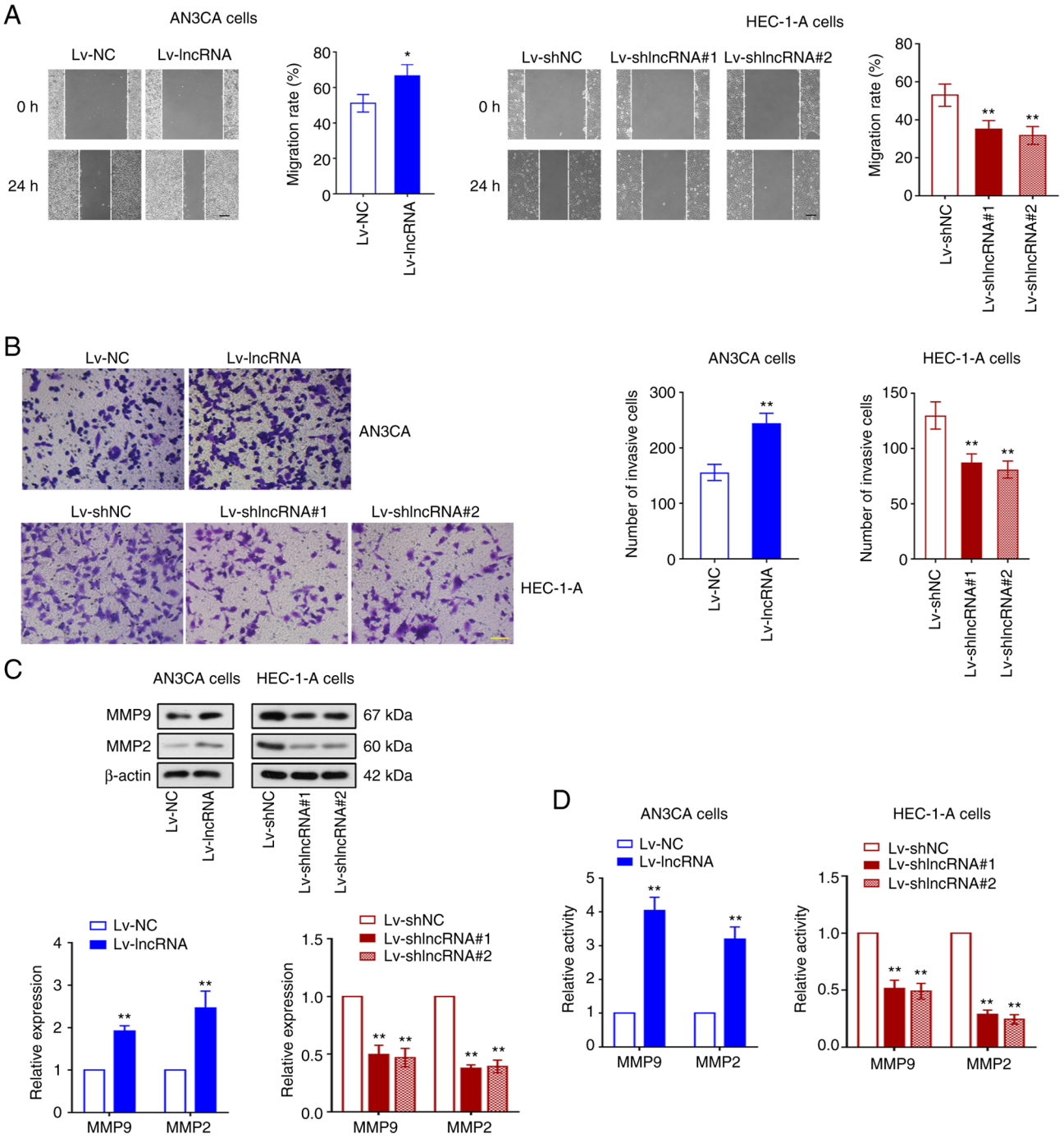

Figure 3. BLACAT2 facilitates UCEC cell migration and invasion. The AN3CA stable cell line with overexpressed BLACAT2 and the HEC-1-A stable cell line with knocked down BLACAT2 were established, respectively, before the migration and invasion of UCEC cells were detected. (A) Migration of AN3CA and HEC-1-A cells was detected by wound healing assay, before the migration rate was calculated. Magnification, x100. Scale bar, 200 μm (B) Invasion of AN3CA and HEC-1-A cells was measured using Transwell assay, before the number of invasive cells was recorded. Magnification, x200. Scale bar, 100 μm. (C) Relative protein expression levels of MMP9 and MMP2 in AN3CA and HEC-1-A cells were measured by western blot analysis. (D) The activities of MMP9 and MMP2 in AN3CA and HEC-1-A cells were determined using gelatin zymography assay. Values are presented as the means ± SD (n=3). *P<0.05 and **P<0.01 vs. Lv-NC or Lv-shNC. BLACAT2, bladder cancer-associated transcript 2; UCEC, uterine corpus endometrial carcinoma; Lv, lentivirus; sh, short-interfering; NC, negative control.

cells (P<0.01; Fig. 4C and D). These results indicated that BLACAT2 can regulate MEK/ERK signaling in UCEC cells.

BLACAT2 promotes UCEC tumor growth in vivo. The effect of BLACAT2 on UCEC progression was next studied *in vivo*. AN3CA cells with stably overexpressed BLACAT2/NC and HEC-1-A cells with stably knocked down BLACAT2/NC, were injected into nude mice. The tumor volumes and weights of the nude mice injected with cells overexpressing BLACAT2 were found to be increased compared with those of nude mice injected with cells expressing Lv-NC. However, BLACAT2 knockdown suppressed tumor growth in nude mice (P<0.05; Fig. 5A-C). The expression of Ki-67 using immunohitochemical (IHC) staining indicated that BLACAT2 overexpression

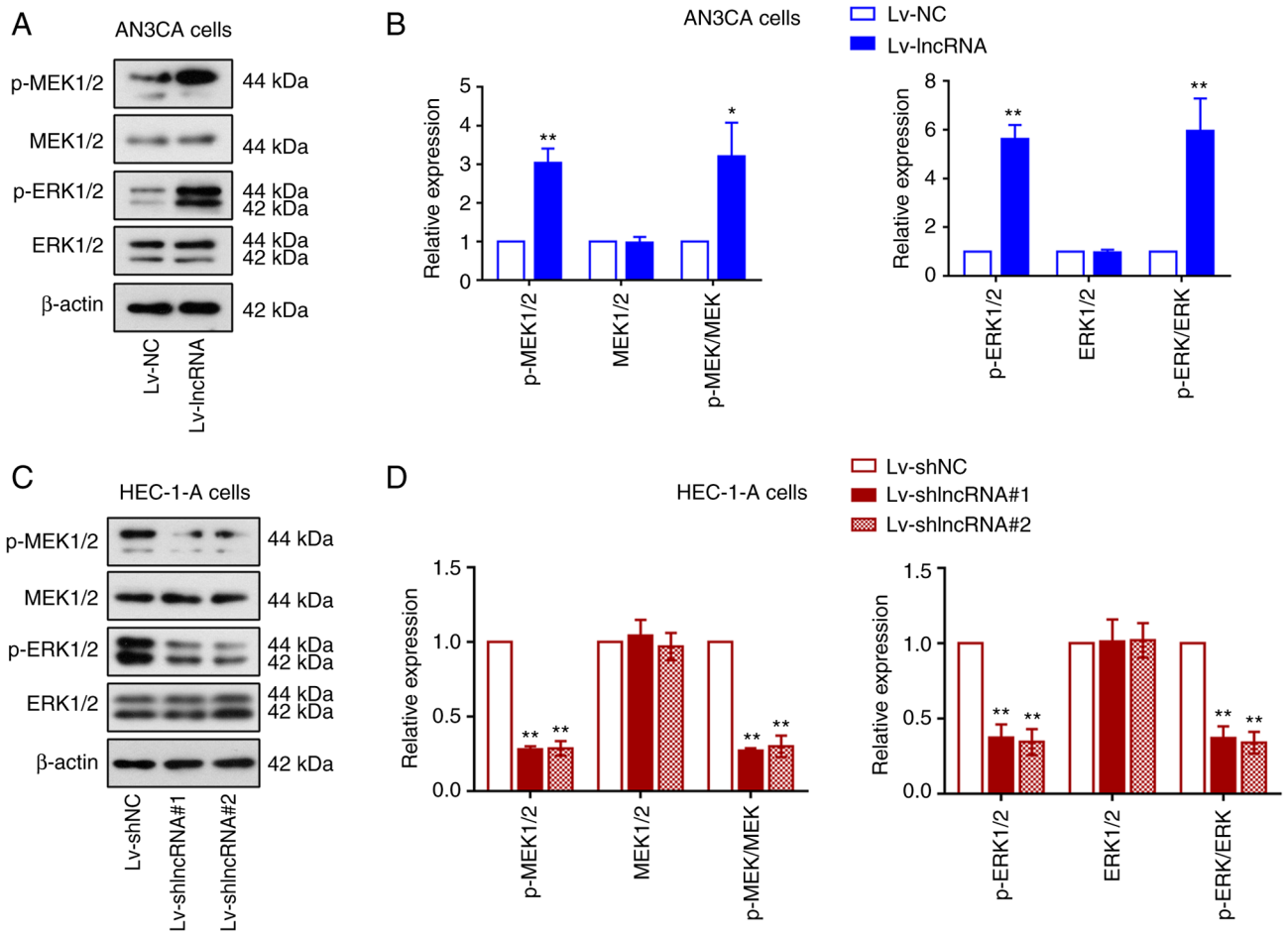

Figure 4. BLACAT2 overexpression enhances MER/ERK signaling in uterine corpus endometrial carcinoma cells. Expression of the protein markers in the MEK/ERK signaling pathway were next analyzed in AN3CA cells with stably overexpressed BLACAT2 and in HEC-1-A cells with stably knocked down BLACAT2. (A) Representative images of western blot analysis of p-MEK1/2, total MEK1/2, p-ERK1/2, and total ERK1/2 both in AN3CA cells, (B) which were semi-quantified. (C) Representative images of western blot analysis of p-MEK1/2, total MEK1/2, p-ERK1/2, and total ERK1/2 both in HEC-1-A cells, (D) which were semi-quantified. Values are presented as the means ± SD (n=3). *P<0.05 and **P<0.01 vs. Lv-NC or Lv-shNC. BLACAT2, bladder cancer-associated transcript 2; p-, phosphorylated; Lv, lentivirus; sh, short-interfering; NC, negative control.

promoted, whereas BLACAT2 knockdown suppressed UCEC tumor cell proliferation (Fig. 5D). Furthermore, the protein expression levels of cyclin D1, MMP2 and phosphorylated ERK1/2 were also increased by BLACAT2 overexpression but inhibited by BLACAT2 knockdown (P<0.01; Fig. 5E and F). These observations indicated that BLACAT2 promoted UCEC tumor growth and activation of MEK/ERK signaling *in vivo*.

Association among BLACAT2, miR-378a-3p, and YY1. The predictive binding among BLACAT2, miR-378a-3p, and YY1 is presented in Fig. 6A. The putative binding sites of BLACAT2 to miR-378a-3p and miR-378a-3p to YY1 3'UTR are shown in Fig. 6B. BLACAT2 overexpression was demonstrated to reduce miR-378a-3p expression, but to increase that of YY1 in UCEC cells, whilst BLACAT2 knockdown exerted the opposite effects (P<0.01; Fig. 6C). BLACAT2 overexpression also led to reduced miR-378a-3p expression and increased YY1 expression in UCEC tumors, whilst BLACAT2 knockdown enhanced miR-378a-3p expression and reduced YY1 expression (P<0.01; Fig. S1). The potential targeted association between miR-378a-3p and BLACAT2 or YY1 was next assessed using dual-luciferase reporter assays. The relative luciferase activity in 293T cells co-transfected with vectors containing wild-type BLACAT2 3'UTR and miR-378a-3p was reduced, suggesting that miR-378a-3p can bind to BLACAT2. miR-378a-3p was also found to bind to the 3'UTR of YY1 (P<0.01; Fig. 6D). In addition, Fig. 6E revealed the possible binding sites of YY1 in the BLACAT2 promoter region. The increased relative luciferase activity in 293T cells co-transfected with the YY1 and BLACAT2 promoter suggested that YY1, as a transcription factor, may bind to the BLACAT2 promoter (Fig. 6E). This was further verified using ChIP assay (Fig. 6F).

miR-378a-3p overexpression inhibits UCEC cell proliferation, invasion and the ERK pathway. To study the function of miR-378a-3p in UCEC cells, HEC-1-A cells were transfected with either miR-378a-3p mimics or NC mimics. The transfection efficiency was validated and is presented in Fig. S2. The mRNA expression level of YY1 in HEC-1-A cells was significantly decreased following miR-378a-3p overexpressin (P<0.01; Fig. 7A). miR-378a-3p overexpression also significantly suppressed the viability and invasion of UCEC cells (P<0.01; Fig. 7B and C). The expression of cyclin D1, MMP2, and ERK1/2 phosphorylation was found to be inhibited by

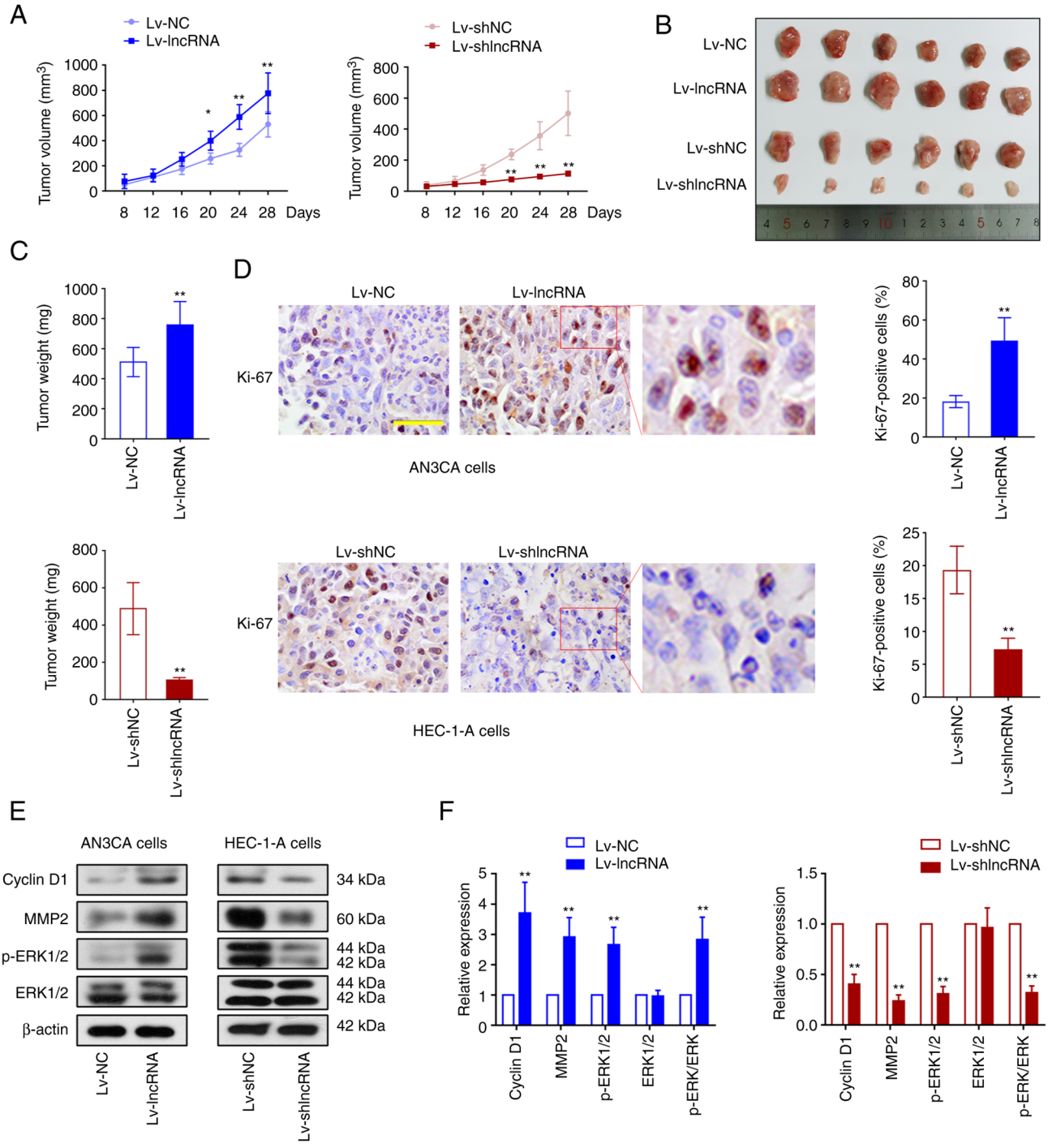

Figure 5. BLACAT2 promotes UCEC tumor growth *in vivo*. AN3CA cells with stably overexpressed BLACAT2 and HEC-1-A cells with stably knocked down BLACAT2 were injected into the right flank of nude mice. (A) The volume of UCEC tumors in nude mice was measured every 4 days. (B) The images of UCEC tumors removed from the nude mice 4 weeks after injection. (C) The weight of the tumors in nude mice was measured after sacrifice. (D) Immunohistochemical staining showed the expression of Ki-67 in the UCEC tumors in nude mice. Magnification, x400. Scale bar, 50 μm. (E) Representative western blotting images and (F) protein expression semi-quantification of cyclin D1, MMP2, phosphorylated ERK1/2 and ERK1/2 in the tumors. Values are presented as the means ± SD (n=6). *P<0.05 and **P<0.01 vs. Lv-NC or Lv-shNC. BLACAT2, bladder cancer-associated transcript 2; UCEC, uterine corpus endometrial carcinoma; Lv, lentivirus; sh, short-interfering; NC, negative control; p-, phosphorylated.

miR-378a-3p overexpression (P<0.01; Fig. 7D), suggesting that miR-378a-3p can suppress cell proliferation, invasion, and ERK signaling in UCEC cells.

YY1 knockdown reverses BLACAT2 overexpression-mediated UCEC development. To investigate whether YY1 is involved in the regulation of BLACAT2 and therefore UCEC development, Lv-shYY1 was used to infect AN3CA cells, and YY1 expression was knocked down effectively in AN3CA cells after the infection (P<0.01; Fig. 8A). AN3CA cells with stably overexpressed BLACAT2 were then infected with Lv-shYY1 or Lv-shNC. CCK-8 assay revealed that in BLACAT2-overexpressed UCEC cells, YY1 down-regulation significantly reduced cell viability (P<0.01;

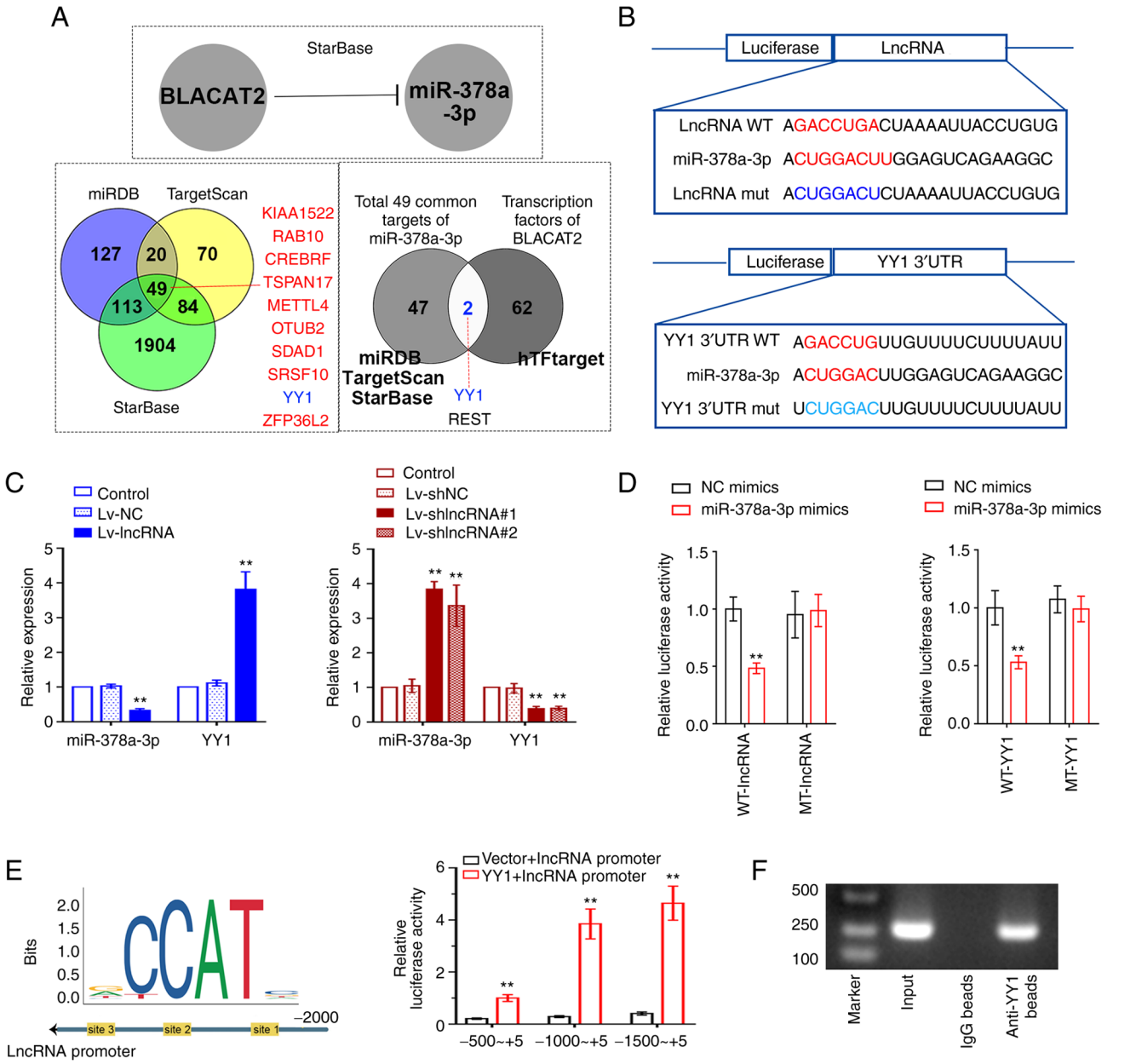

Figure 6. Association among BLACAT2, miR-378a-3p and YY1. (A) starBase predicted the binding of BLACAT2 and miR-378a-3p. Venn diagram of the potential targets of miR-378a-3p was produced after prediction using miRDB, TargetScan and starBase. Venn diagram showing a total of 49 common possible targets of miR-378a-3p and the potential transcription factors of BLACAT2 were predicted by Jasper. (B) Wild-type putative sites of BLACAT2 or the YY1 3'UTR or their corresponding mutant sequences were cloned into the pmirGLO luciferase reporter vector. (C) Relative expression of miR-378-3p and YY1 in AN3CA cells with stably overexpressed BLACAT2 and in HEC-1-A cells with stably knocked down BLACAT2. (D) Relative luciferase activity of 293T cells was detected to assess the association between miR-378a-3p and BLACAT2 or the YY1 3'UTR. (E) In total, three different regions in the BLACAT2 promoter were selected and cloned into the pmirGLO vector, before luciferase reporter assays were performed to investigate the possible binding between the YY1 and BLACAT2 promoter. (F) ChIP analysis of YY1 binding to the BLACAT2 promoter. After ChIP, the PCR products were analyzed by gel electrophoresis. Values are presented as the means ± SD (n=3). **P<0.01 vs. Lv-NC, Lv-shNC, NC mimics or Vector + BLACAT2 promoter. BLACAT2, bladder cancer-associated transcript 2; miR, microRNA; YY1, Yin Yang-1; UTR, untranslated region; ChIP, chromatin immunoprecipitation; Lv, lentivirus; sh, short-interfering; NC, negative control; WT-, wild-type; MT-mutant.

Fig. 8B). In addition, YY1 knockdown abrogated the positive effects of BLACAT2 on UCEC cell migration and invasion (P<0.05; Fig. 8C and D). The protein expression levels of cyclin D1, MMP2 and ERK1/2 phosphorylation were also significantly supressed by YY1 inhibition (P<0.01; Fig. 8E and F). These results indicated that YY1 is involved in the regulation of BLACAT2 expression upstream of UCEC cell proliferation, migration, invasion, and MER/ERK signaling.

Discussion

In the present study, BLACAT2 overexpression was found to promote UCEC cell proliferation, migration, and invasion. The tumor-promoting effects of BLACAT2 in UCEC are likely to be mediated by a miR-378a-3p/YY1 axis. This BLACAT2/miR-378a-3p/YY1 axis in UCEC development is also likely to involve the MEK/ERK signaling pathway. In addition, YY1 may bind to the promoter of BLACAT2 to regulate its expression.

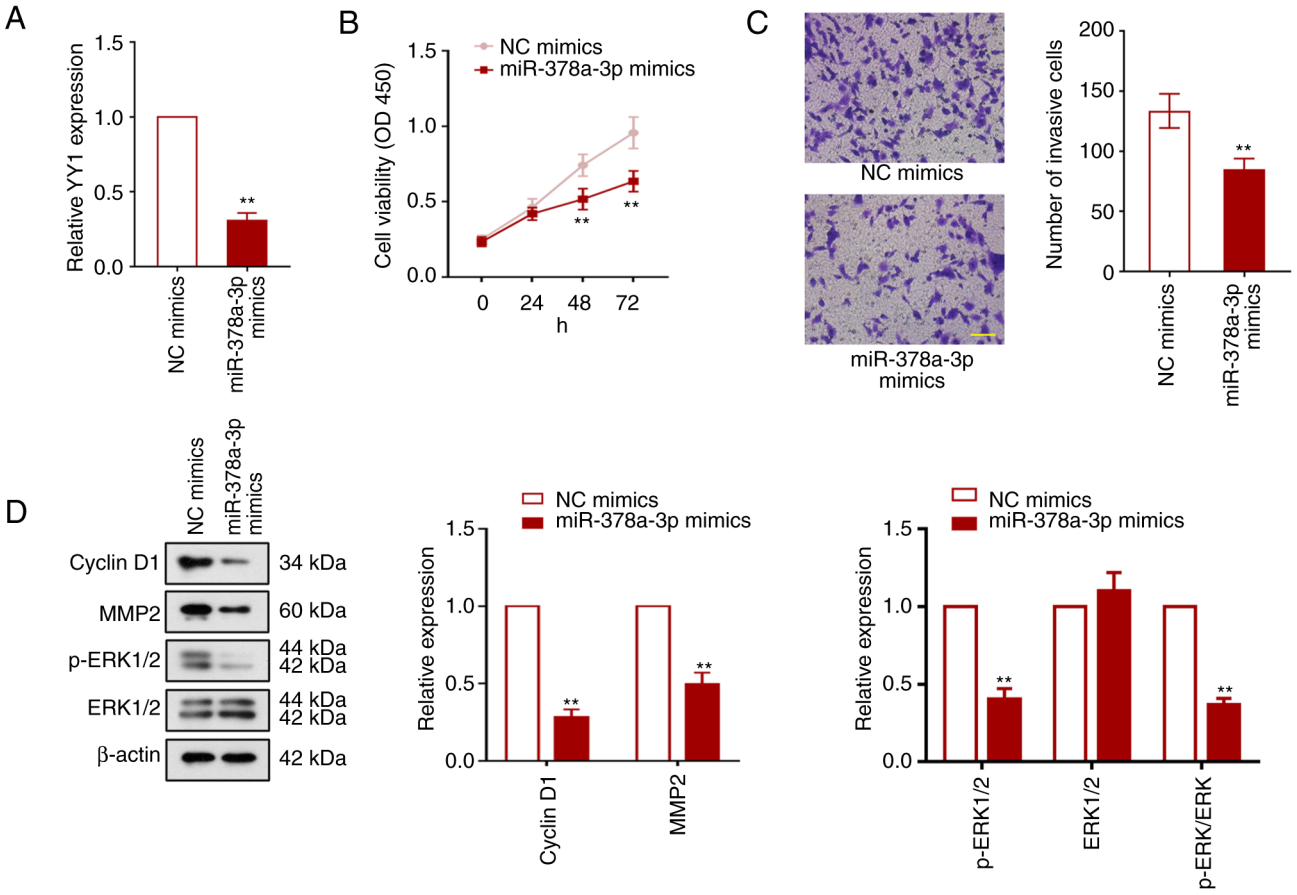

Figure 7. miR-378a-3p overexpression inhibits UCEC cell proliferation, invasion and the ERK1/2 pathway. HEC-1-A cells were transfected with the miR-378a-3p mimics to explore the function of miR-378a-3p in UCEC progression. (A) Relative expression of Yin Yang-1 in HEC-1-A cells was detected using reverse transcription-quantitative PCR 48 h after transfection. (B) Cell viability was measured using the Cell Counting Kit-8 assay. (C) The effect of miR-378a-3p overexpression on HEC-1-A cell invasion. Magnification, x200. Scale bar, 100 μm (D) Relative expression levels of cyclin D1, mature MMP2, ERK1/2 and phosphorylated ERK1/2 in HEC-1-A cells. Values are presented as the means ± SD (n=3). **P<0.01 vs. NC mimics. miR, microRNA; UCEC, uterine corpus endometrial carcinoma; YY1, Yin Yang-1; NC, megative control; p-, phosphorylated.

LncRNAs are expressed in a tissue- and cell-type-specific manner, where they have been demonstrated to serve vital roles in multiple cancers (43,44). A previous study identified seven lncRNAs to be potential prognostic factors in UCEC according to RNA-sequencing and expression profiling coupled with analysis of corresponding clinical data of patients with UCEC from The Cancer Genome Atlas database (45). Illumina paired-end RNA sequencing demonstrated that BLACAT2 expression is upregulated in endometrial, ovarian and cervical cancer (20). BLACAT2 has been found to be differently expressed in UCEC tumor and normal tissue, but its function and mechanism in UCEC remain poorly understood. In the present study, BLACAT2 overexpression was found to suppress miR-378a-3p expression, whilst promoting YY1 expression, UCEC cell viability, cell cycle progression, cell migration and invasion. By contrast, BLACAT2 knockdown exerted the opposite effects on all of the aforementioned physiological processes. As part of the cyclin family of proteins, cyclin D1 and cyclin E are important regulators of cancer cell proliferation, the downregulation of which was associated with cell cycle arrest (46,47). By contrast, the migration and invasion of cancer cells are mediated by metalloproteinases, MMP2 and MMP9 (48,49). The present study revealed increased cyclin D1, cyclin E, MMP2, and MMP9 in UCEC cells following BLACAT2 overexpression, whereas they were all reduced by BLACAT2 knockdown. This suggests that BLACAT2 overexpression can promote UCEC cell proliferation, migration, and invasion. In addition, it was found that the BLACAT2-mediated UCEC cell proliferation was associated with increases in p-MEK/MEK and p-ERK/ERK ratios, suggesting that BLACAT2 overexpression can also activate MEK/ERK signaling in UCEC cells. The tumor-promoting effects of the activated MEK/ERK pathway have been demonstrated in previous studies (50,51). Therefore, the results from the present study revealed a potential novel signaling pathway regulated by BLACAT2 in UCEC.

LncRNAs typically function as competing endogenous RNAs with other RNA transcripts for the same miRNAs (52). LncRNAs can function as miRNA sponges and block the regulatory effects of miRNAs on mRNAs (53). The regulation of transcription is a complex process that involves interactions among different types of signaling components, including mRNA, lncRNA and miRNA. Liu *et al* (54) previously proposed a novel method for constructing genome-wide interactive networks and found the cross-regulation of lncRNA, miRNA and mRNA, called the 'mRNA-lncRNA-miRNA triplet'. miR-378a-3p was predicted to bind to BLACAT2 using bioinformatic analysis, which was then confirmed

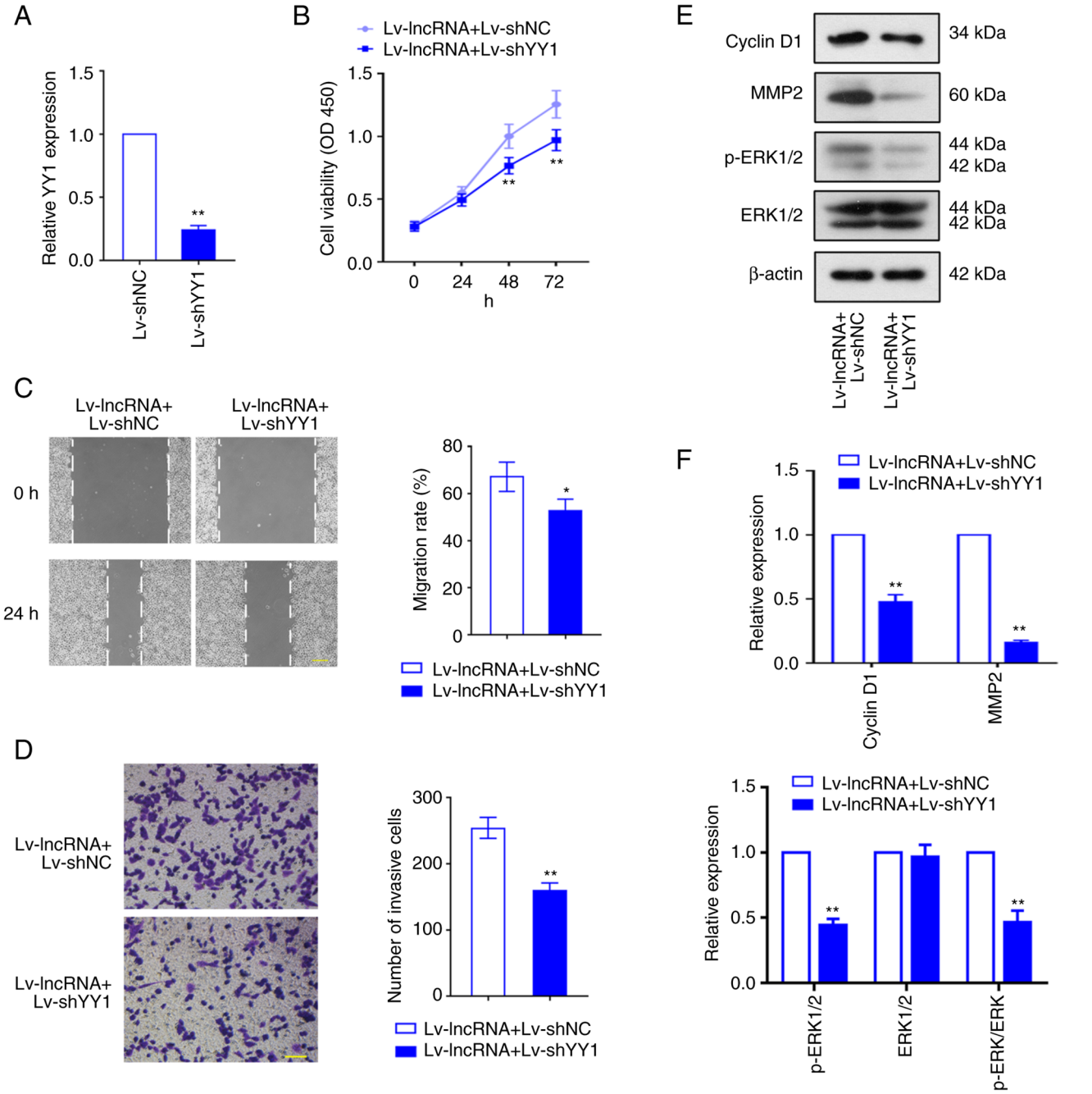

Figure 8. YY1 knockdown inhibits BLACAT2 overexpression-mediated uterine corpus endometrial carcinoma development. Lentiviruses encoding shYY1 (Lv-shYY1) were used to infect AN3CA cells with stably overexpressed BLACAT2. (A) The infectivity of the shYY1 lentivirus (Lv-shYY1) was verified in AN3CA cells. (B) The viability of AN3CA cells was determined using Cell Counting Kit-8 assay. (C) Migration of AN3CA cells was detected using a wound healing assay, before the migration rate was calculated. Magnification, x100. Scale bar, 200 μm. (D) The effect of YY1 knockdown on AN3CA cell invasion following BLACAT2 overexpression. Magnification, x200. Scale bar, 100 μm. (E) Representative images and (F) semi-quantification of protein expression of cyclin D1, MMP2, phosporylated ERK1/2 and total ERK1/2 in AN3CA cells after transfection. Values are presented as the means ± SD (n=3). *P<0.05 and **P<0.01 vs. Lv-BLACAT2 + Lv-shNC. YY1, Yin Yang-1; BLACAT2, bladder cancer-associated transcript 2; sh, short-interfering; Lv, lentivirus; NC, negative control; p-, phosphorylated.

using a dual-luciferase report assay. The interaction of BLACAT2 with miR-378a-3p was also found in a previous study by Cui *et al* (35), which demonstrated that BLACAT2 can regulate cancer development by sponging miR-378a-3p. Previous studies demonstrated that tumor promotion may involve miR-378a-3p inhibition (55,56). In the present study, miR-378a-3p overexpression resulted in the suppression of YY1 expression, UCEC cell proliferation and invasion, suggesting the antitumor role of miR-378a-3p in UCEC. Hu *et al* (16) previously showed that BLACAT2 can serve as an oncogene by modulating the miR-193b-5p/methyltransferase 3, N6-adenosine-methyltransferase complex catalytic subunit axis (16). In the present study, the function of BLACAT2 in UCEC progression may be achieved by the regulation of miR-378a-3p and YY1 downstream, which further affected the MEK/ERK pathway. Therefore, the differential roles of BLACAT2 in human cancers may depend on its different downstream miRNAs and target mRNAs.

YY1 was shown to be a potential target of miR-378a-3p. YY1 was previously found to be overexpressed in tumors and identified to be an oncogenic factor. This was potentially mediated by the recruitment of enhancer of zeste homolog 2 and the activation of histone H3K27me3 in the adenomatous polyposis coli gene promoter region in EEC, which silences the expression of this gene. In addition, YY1 depletion was found to suppress EEC cell proliferation and migration, whilst YY1 overexpression could promote these processes (30). YY1 can also function as a positive regulator of AKT1, a member of the PI3K/AKT/mTOR signaling pathway activated in endometrial tumors (57). These previous studies suggest that YY1 is an important regulator of endometrial carcinoma progression. Consistently, the present study showed that YY1 knockdown abolished the BLACAT2 overexpression-induced UCEC cell proliferation, invasion and activation of MEK/ERK signaling, suggesting that YY1 was involved in the regulation of BLACAT2 and therefore UCEC progression. In gastric cancer cells, YY1 knockdown resulted in the inhibition of ERK/MAPK signaling, a major oncogenic pathway (58). Therefore, the present study revealed that the induction of YY1 expression may activate the ERK pathway to promote UCEC tumor growth.

The direct binding of YY1 to the gene promoter of BLACAT2 was identified using dual-luciferase reporter and ChIP assays in the present study, suggesting that YY1 can regulate BLACAT2 transcription. The regulatory relationship among BLACAT2, miR-378a-3p, and YY1 appears to form a feedback loop instead of an axis. Therefore, BLACAT2 not only controls UCEC development by regulating the miR-378a-3p/YY1 axis, but is also under the control of the transcription factor YY1. Based on these findings, BLACAT2 may bind to miR-378a-3p and function as a sponge of this miRNA, resulting in the abolishment of the inhibitory effects of miR-378a-3p on YY1 in UCEC. However, the regulatory mechanism of YY1 in BLACAT2 expression requires further investigation. In addition, the association of the BLACAT2/miR-378a-3p/YY1 loop with the ERK signaling pathway in UCEC cells warrants further exploration in the future.

Findings from the present study suggest the potential of BLACAT2 as a biomarker in UCEC. However, the present study also has various limitations. It is essential to enroll an increased number of cancer cases in future studies. In addition, the majority of lncRNAs can regulate >1 target gene, but only the preliminary regulatory mechanism of the effect of BLACAT2 was revealed in the present study. The specific mechanisms involved in the effect of BLACAT2 in UCEC require further investigation. Furthering the understanding of the function and potential molecular mechanisms of BLACAT2 will facilitate the development of lncRNA-based therapeutics in the clinic.

In conclusion, in the present study it was revealed that BLACAT2 regulated the progression of UCEC through the miR-378a-3p/YY1 axis. However, downstream YY1 can bind to BLACAT2 promoter to promote its expression as a transcription factor. In addition, MEK/ERK is involved downsteam of the BLACAT2/miR-378a-3p/YY1 loop in UCEC progression. The present study therefore provides novel therapeutic targets for UCEC and insights into UCEC tumorigenesis.

Acknowledgements

Not applicable.

Funding

The present study was supported by the Public Health Research and Development Project of Shenyang (Medical Technology Improvement Project of Common Multiple Diseases), grant no. 22-321-33-15.

Availability of data and materials

The data used to support the findings of this study are included in the manuscript.

Authors' contributions

CZ and QY conceived and designed the experiments. CZ and RW performed the experiments. CZ, RW and ML analyzed the data, and performed the bioinformatics analysis. CZ wrote the manuscript. QY helped edit the manuscript. CZ and QY confirm the authenticity of all the raw data. All authors read and approved the final manuscript.

Ethics approval and consent to participate

The research protocol was approved (approval no. 2021PS723K) by the Ethics Committee of Shengjing Hospital of China Medical University (Shenyang, China) and was in accordance with the Declaration of Helsinki. The informed consent was obtained from all volunteers. Animal experimental procedures were approved (approval no. 2021PS741K) by the Animal Ethics Committee of Shengjing Hospital of China Medical University.

Patient consent for publication

Not applicable.

Competing interests

The authors declare that they have no competing interests.

References

1. Ferlay J, Soerjomataram I, Dikshit R, Eser S, Mathers C, Rebelo M, Parkin DM, Forman D and Bray F: Cancer incidence and mortality worldwide: sources, methods and major patterns in GLOBOCAN 2012. Int J Cancer 136: E359-E386, 2015.
2. Morice P, Leary A, Creutzberg C, Abu-Rustum N and Darai E: Endometrial cancer. Lancet 387: 1094-1108, 2016.
3. Aoki Y, Kanao H, Wang X, Yunokawa M, Omatsu K, Fusegi A and Takeshima N: Adjuvant treatment of endometrial cancer today. Jpn J Clin Oncol 50: 753-765, 2020.
4. Siegel R, Ma J, Zou Z and Jemal A: Cancer statistics, 2014. CA Cancer J Clin 64: 9-29, 2014.
5. Slavoff SA, Mitchell AJ, Schwaid AG, Cabili MN, Ma J, Levin JZ, Karger AD, Budnik BA, Rinn JL and Saghatelian A: Peptidomic discovery of short open reading frame-encoded peptides in human cells. Nat Chem Biol 9: 59-64, 2013.
6. Cesana M, Cacchiarelli D, Legnini I, Santini T, Sthandier O, Chinappi M, Tramontano A and Bozzoni I: A long noncoding RNA controls muscle differentiation by functioning as a competing endogenous RNA. Cell 147: 358-369, 2011.

7. Bhan A and Mandal SS: Long noncoding RNAs: Emerging stars in gene regulation, epigenetics and human disease. ChemMedChem 9: 1932-1956, 2014.
8. Bhan A, Soleimani M and Mandal SS: Long noncoding RNA and cancer: A new paradigm. Cancer Res 77: 3965-3981, 2017.
9. Seitz AK, Christensen LL, Christensen E, Faarkrog K, Ostenfeld MS, Hedegaard J, Nordentoft I, Nielsen MM, Palmfeldt J, Thomson M, *et al*: Profiling of long non-coding RNAs identifies LINC00958 and LINC01296 as candidate oncogenes in bladder cancer. Sci Rep 7: 395, 2017.
10. He W, Zhong G, Jiang N, Wang B, Fan X, Chen C, Chen X, Huang J and Lin T: Long noncoding RNA BLACAT2 promotes bladder cancer-associated lymphangiogenesis and lymphatic metastasis. J Clin Invest 128: 861-875, 2018.
11. Zuo X, Chen Z, Gao W, Zhang Y, Wang J, Wang J, Cao M, Cai J, Wu J and Wang X: M6A-mediated upregulation of LINC00958 increases lipogenesis and acts as a nanotherapeutic target in hepatocellular carcinoma. J Hematol Oncol 13: 5, 2020.
12. Zhao H, Zheng GH, Li GC, Xin L, Wang YS, Chen Y and Zheng XM: Long noncoding RNA LINC00958 regulates cell sensitivity to radiotherapy through RRM2 by binding to microRNA-5095 in cervical cancer. J Cell Physiol 234: 23349-23359, 2019.
13. Chen M, Xu Z, Zhang Y and Zhang X: LINC00958 promotes the malignancy of nasopharyngeal carcinoma by sponging microRNA-625 and thus upregulating NUAK1. Onco Targets Ther 12: 9277-9290, 2019.
14. Chen S, Chen JZ, Zhang JQ, Chen HX, Qiu FN, Yan ML, Tian YF, Peng CH, Shen BY, Chen YL and Wang YD: Silencing of long noncoding RNA LINC00958 prevents tumor initiation of pancreatic cancer by acting as a sponge of microRNA-330-5p to down-regulate PAX8. Cancer Lett 446: 49-61, 2019.
15. Luo Z, Han Z, Shou F, Li Y and Chen Y: LINC00958 accelerates cell proliferation and migration in non-small cell lung cancer through JNK/c-JUN signaling. Hum Gene Ther Methods 30: 226-234, 2019.
16. Hu H, Kong Q, Huang XX, Zhang HR, Hu KF, Jing Y, Jiang YF, Peng Y, Wu LC, Fu QS, *et al*: Longnon-coding RNA BLACAT2 promotes gastric cancer progression via the miR-193b-5p/METTL3 pathway. J Cancer 12: 3209-3221, 2021.
17. Ren Y, Zhao C, He Y, Xu H and Min X: Long non-coding RNA bladder cancer-associated transcript 2 contributes to disease progression, chemoresistance and poor survival of patients with colorectal cancer. Oncol Lett 18: 2050-2058, 2019.
18. Zhu J, Zhu Z, Cai P, Gu Z and Wang J: Bladder cancer-associated transcript 2 contributes to nephroblastoma progression. J Gene Med 24: e3292, 2022.
19. Binang HB, Wang YS, Tewara MA, Du L, Shi S, Li N, Nsenga AGA and Wang C: Expression levels and associations of five long non-coding RNAs in gastric cancer and their clinical significance. Oncol Lett 19: 2431-2445, 2020.
20. Chen BJ, Byrne FL, Takenaka K, Modesitt SC, Olzomer EM, Mills JD, Farrell R, Hoehn KL and Janitz M: Transcriptome landscape of long intergenic non-coding RNAs in endometrial cancer. Gynecol Oncol 147: 654-662, 2017.
21. Jiang Y, Qiao Z, Jiang J and Zhang J: LINC00958 promotes endometrial cancer cell proliferation and metastasis by regulating the miR-145-3p/TCF4 axis. J Gene Med 23: e3345, 2021.
22. Khachigian LM: The Yin and Yang of YY1 in tumor growth and suppression. Int J Cancer 143: 460-465, 2018.
23. Sarvagalla S, Kolapalli SP and Vallabhapurapu S: The two sides of YY1 in cancer: A friend and a foe. Front Oncol 9: 1230, 2019.
24. Thomas MJ and Seto E: Unlocking the mechanisms of transcription factor YY1: Are chromatin modifying enzymes the key? Gene 236: 197-208, 1999.
25. Qiao K, Ning S, Wan L, Wu H, Wang Q, Zhang X, Xu S and Pang D: LINC00673 is activated by YY1 and promotes the proliferation of breast cancer cells via the miR-515-5p/MARK4/Hippo signaling pathway. J Exp Clin Cancer Res 38: 418, 2019.
26. Berchuck A, Iversen ES, Lancaster JM, Pittman J, Luo J, Lee P, Murphy S, Dressman HK, Febbo PG, West M, *et al*: Patterns of gene expression that characterize long-term survival in advanced stage serous ovarian cancers. Clin Cancer Res 11: 3686-3696, 2005.
27. Seligson D, Horvath S, Huerta-Yepez S, Hanna S, Garban H, Roberts A, Shi T, Liu X, Chia D, Goodglick L and Bonavida B: Expression of transcription factor Yin Yang 1 in prostate cancer. Int J Oncol 27: 131-141, 2005.
28. Luo J, Zhou X, Ge X, Liu P, Cao J, Lu X, Ling Y and Zhang S: Upregulation of Ying Yang 1 (YY1) suppresses esophageal squamous cell carcinoma development through heme oxygenase-1. Cancer Sci 104: 1544-1551, 2013.
29. Zhao G, Li Q, Wang A and Jiao J: YY1 regulates melanoma tumorigenesis through a miR-9~RYBP axis. J Exp Clin Cancer Res 34: 66, 2015.
30. Yang Y, Zhou L, Lu L, Wang L, Li X, Jiang P, Chan LK, Zhang T, Yu J, Kwong J, *et al*: A novel miR-193a-5p-YY1-APC regulatory axis in human endometrioid endometrial adenocarcinoma. Oncogene 32: 3432-3442, 2013.
31. Masood N, Basharat Z, Khan T and Yasmin A: Entangling relation of micro RNA-let7, miRNA-200 and miRNA-125 with various cancers. Pathol Oncol Res 23: 707-715, 2017.
32. Xiao M, Iglinski-Benjamin KC, Sharpe O, Robinson WH and Abrams GD: Exogenous micro-RNA and antagomir modulate osteogenic gene expression in tenocytes. Exp Cell Res 378: 119-123, 2019.
33. Jiang T, Sui D, You D, Yao S, Zhang L, Wang Y, Zhao J and Zhang Y: MiR-29a-5p inhibits proliferation and invasion and induces apoptosis in endometrial carcinoma via targeting TPX2. Cell Cycle 17: 1268-1278, 2018.
34. Wang P, Zeng Z, Shen X, Tian X and Ye Q: Identification of a multi-RNA-type-based signature for recurrence-free survival prediction in patients with uterine corpus endometrial carcinoma. DNA Cell Biol 39: 615-630, 2020.
35. Cui Y, Xie M and Zhang Z: LINC00958 involves in bladder cancer through sponging miR-378a-3p to elevate IGF1R. Cancer Biother Radiopharm 35: 776-788, 2020.
36. Livak KJ and Schmittgen TD: Analysis of relative gene expression data using real-time quantitative PCR and the 2(-Delta Delta C(T)) method. Methods 25: 402-408, 2001.
37. Thomas GJ, Lewis MP, Hart IR, Marshall JF and Speight PM: AlphaVbeta6 integrin promotes invasion of squamous carcinoma cells through up-regulation of matrix metalloproteinase-9. Int J Cancer 92: 641-650, 2001.
38. Wang L, Zhong Y, Yang B, Zhu Y, Zhu X, Xia Z, Xu J and Xu L: LINC00958 facilitates cervical cancer cell proliferation and metastasis by sponging miR-625-5p to upregulate LRRC8E expression. J Cell Biochem 121: 2500-2509, 2020.
39. Xie M, Fu Q, Wang PP and Cui YL: STAT1-induced upregulation lncRNA LINC00958 accelerates the epithelial ovarian cancer tumorigenesis by regulating Wnt/β-catenin signaling. Dis Markers 2021: 1405045, 2021.
40. Zhang D, Ma Q, Wang Z, Zhang M, Guo K, Wang F and Wu E: β2-adrenoceptor blockage induces G1/S phase arrest and apoptosis in pancreatic cancer cells via Ras/Akt/NFκB pathway. Mol Cancer 10: 146, 2011.
41. Sato H, Takino T, Okada Y, Cao J, Shinagawa A, Yamamoto E and Seiki M: A matrix metalloproteinase expressed on the surface of invasive tumour cells. Nature 370: 61-65, 1994.
42. Roberts PJ and Der CJ: Targeting the Raf-MEK-ERK mitogen-activated protein kinase cascade for the treatment of cancer. Oncogene 26: 3291-3310, 2007.
43. Fatima R, Akhade VS, Pal D and Rao SM: Long noncoding RNAs in development and cancer: Potential biomarkers and therapeutic targets. Mol Cell Ther 3: 5, 2015.
44. Cheetham SW, Gruhl F, Mattick JS and Dinger ME: Long noncoding RNAs and the genetics of cancer. Br J Cancer 108: 2419-2425, 2013.
45. Ouyang D, Li R, Li Y and Zhu X: A 7-lncRNA signature predict prognosis of uterine corpus endometrial carcinoma. J Cell Biochem 120: 18465-18477, 2019.
46. Yuan C, Zhu X, Han Y, Song C, Liu C, Lu S, Zhang M, Yu F, Peng Z and Zhou C: Elevated HOXA1 expression correlates with accelerated tumor cell proliferation and poor prognosis in gastric cancer partly via cyclin D1. J Exp Clin Cancer Res 35: 15, 2016.
47. Park GH, Song HM and Jeong JB: The coffee diterpene kahweol suppresses the cell proliferation by inducing cyclin D1 proteasomal degradation via ERK1/2, JNK and GKS3β-dependent threonine-286 phosphorylation in human colorectal cancer cells. Food Chem Toxicol 95: 142-148, 2016.
48. Liu H, Zeng Z, Wang S, Li T, Mastriani E, Li QH, Bao HX, Zhou YJ, Wang X, Liu Y, *et al*: Main components of pomegranate, ellagic acid and luteolin, inhibit metastasis of ovarian cancer by down-regulating MMP2 and MMP9. Cancer Biol Ther 18: 990-999, 2017.
49. Wang X, Yang B, She Y and Ye Y: The lncRNA TP73-AS1 promotes ovarian cancer cell proliferation and metastasis via modulation of MMP2 and MMP9. J Cell Biochem 119: 7790-7799, 2018.

50. Wang Y, Zhu Y, Zhang L, Tian W, Hua S, Zhao J, Zhang H and Xue F: Insulin promotes proliferation, survival, and invasion in endometrial carcinoma by activating the MEK/ERK pathway. Cancer Lett 322: 223-231, 2012.
51. Wang F, Chen Q, Huang G, Guo X, Li N, Li Y and Li B: BKCa participates in E2 inducing endometrial adenocarcinoma by activating MEK/ERK pathway. BMC Cancer 18: 1128, 2018.
52. Zhao Z, Sun W, Guo Z, Zhang J, Yu H and Liu B: Mechanisms of lncRNA/microRNA interactions in angiogenesis. Life Sci 254: 116900, 2020.
53. Paraskevopoulou MD and Hatzigeorgiou AG: Analyzing MiRNA-LncRNA interactions. Methods Mol Biol 1402: 271-286, 2016.
54. Liu C, Zhang YH, Deng Q, Li Y, Huang T, Zhou S and Cai YD: Cancer-related triplets of mRNA-lncRNA-miRNA revealed by integrative network in uterine corpus endometrial carcinoma. Biomed Res Int 2017: 3859582, 2017.
55. Kong D, Hou Y, Li W, Ma X and Jiang J: LncRNA-ZXF1 regulates P21 expression in endometrioid endometrial carcinoma by managing ubiquitination-mediated degradation and miR-378a-3p/PCDHA3 axis. Mol Oncol 16: 813-829, 2021.
56. Rong D, Dong Q, Qu H, Deng X, Gao F, Li Q and Sun P: m^6A-induced LINC00958 promotes breast cancer tumorigenesis via the miR-378a-3p/YY1 axis. Cell Death Discov 7: 27, 2021.
57. Painter JN, Kaufmann S, O'Mara TA, Hillman KM, Sivakumaran H, Darabi H, Cheng THT, Pearson J, Kazakoff S, Waddell N, *et al*: A common variant at the 14q32 endometrial cancer risk locus activates AKT1 through YY1 binding. Am J Hum Genet 98: 1159-1169, 2016.
58. Bhaskar Rao D, Panneerpandian P, Balakrishnan K and Ganesan K: YY1 regulated transcription-based stratification of gastric tumors and identification of potential therapeutic candidates. J Cell Commun Signal 15: 251-267, 2021.